Impact of nanosecond repetitively pulsed electric discharges on the ignition of methane-air mixture

M. Castela[a,b,*], B. Fiorina[a,b], A. Coussement[a,b], O. Gicquel[a,b], N. Darabiha[a,b], C. Laux[a,b]

[a] *Ecole Centrale Paris, Grande Voie des Vignes, 92290 Châtenay-Malabry, France*
[b] *CNRS, UPR 288, Laboratoire d'Energétique Moléculaire et Macroscopique, Combustion (EM2C), Grande Voie des Vignes, 92290 Châtenay-Malabry, France*

Abstract

This article presents an analytical model to describe plasma discharges effects on gas temperature and species dissociation that control autoignition in reactive systems. The model is constructed based on experimental and numerical results of Nanosecond Repetitively Pulsed (NRP) discharges in air and evaluated against the existing experimental data. The model is fully coupled with multi-dimensional flow balance equations where detailed transport coefficients and chemical kinetic mechanism are considered. Sequence of discharge pulses in air and methane-air mixture are computed by means of Direct Numerical Simulations in quiescent and turbulent flow configurations. Gas temperature, pressure and O atoms evolution during NRP discharges in air are in good agreement with experimental results. Ignition phenomenon through NRP discharges of a methane-air mixture is analyzed. The results show an accumulation of vibrational energy in the vicinity of the discharge zone due to the former discharges prior to mixture ignition. This discharge energy stored as gas vibrational energy seems to play a minor role on the ignition process initiation. The early production of O atoms during the discharge favors the initial chain branching reactions, increasing the concentration of radicals in the vicinity of the discharge zone. The initial conditions of turbulence, such as Reynolds number, inside the discharge zone impacts on the number of pulses needed to ignite the mixture.

Keywords: Plasma-assisted combustion, ignition model, premixed combustion, nanosecond repetitively pulsed discharge, plasma turbulence

1. Introduction

Plasma-assisted combustion is rising the interest of both plasma and combustion communities. As demonstrated in several experimental works [1, 2, 3, 4] Nanosecond Repetitively Pulsed (NRP) discharges may be placed as an efficient technique to initiate and control combustion processes, where conventional ignition systems are rather ineffective or extremely energy costly [4]. Recent experiments have shown that both flame stabilization and ignition phenomena become more efficient if this kind of discharges are applied. Although it may look a promising technique, the phenomena occurring in NRP discharges-assisted combustion are still not well understood. Two major questions arise, the first concerns the role of the gas temperature and excited molecules induced by the plasma discharge on combustion enhancement, and the second concerns the impact of turbulence during the process. In order to understand the first question, coupled plasma and combustion detailed kinetic simulations have been used in several numerical works. The vast majority of these numerical studies are 0-D and 1-D simulations. Nevertheless, the problem complexity increases, in practical ignition phenomenon. Indeed, as kernels formed at each pulse are also likely to be controlled by the flow and mixing field. Radicals created at each pulse may favours initial chain branching reactions increasing the local concentration of intermediate species, while turbulence, on the other hand, tends to diffuse and convect these radicals around the discharge zone. In repetitively pulsed regime, there is a competition between NRP discharges and elementary branching reactions characteristic scales (time and space) from one side, and the characteristic scales of turbulence from the other. The aim of the present work is to study the influence of transport phenomena on NRP discharges-assisted ignition. A Direct Numerical Simulation (DNS) taking into account both plasma and combustion detailed kinetics and high turbulent Reynolds number, as such of practical configurations, still remains out of reach due to high CPU cost. Therefore, a low CPU cost analytical strategy is developed to model the impact of the electric discharge on gas temperature and species dissociation at each pulse. The model is constructed based on experimental and numerical observations of this kind of discharges. In the following sections we first describe the set of classical governing equations of a reactive system. These governing equations are then modified according to the proposed NRP model. With this, a series of feasible multi-dimensional numeric studies comprising both detailed transport coefficients and hydrocarbons-air chemistry is pursued. Model results are evaluated against available results in literature for NRP discharges in air. Ignition phenomenon through NRP discharges of a methane-air mixture is analysed in both quiescent and turbulent flow conditions.

*Corresponding author : maria.castela@ecp.fr

2. Governing Equations and NRP discharge model description

2.1. Governing equations

The set of classical equations governing a reactive system, where N_{sp} species are in thermal equilibrium, can be written as:

$$\frac{\partial \rho}{\partial t} + \frac{\partial(\rho u_i)}{\partial x_i} = 0 \tag{1}$$

$$\frac{\partial(\rho u_j)}{\partial t} + \frac{\partial(\rho u_i u_j)}{\partial x_i} = -\frac{\partial p}{\partial x_j} + \frac{\partial \tau_{ij}}{\partial x_i} \tag{2}$$

$$\frac{\partial(\rho Y_k)}{\partial t} + \frac{\partial}{\partial x_i}(\rho(u_i + V_{k,i})Y_k) = W_k \dot{\omega}_k^c \tag{3}$$

$$\frac{\partial(\rho e)}{\partial t} + \frac{\partial(\rho u_i e)}{\partial x_i} = -\frac{\partial q_i}{\partial x_i} + \frac{\partial}{\partial x_i}(\sigma_{ij} u_i) \tag{4}$$

In these equations, ρ is the density, u_i the velocity component in x_i spatial direction, p the pressure. τ_{ij} refers to the viscous tensor. Y_k is the k^{th} species mass fraction. The diffusion velocity of the k^{th} species, $V_{k,i}$, is computed assuming mixture average transport phenomena as in [5]. $\dot{\omega}_k^c$ represents the molar production rate of the k^{th} species due to combustion. The energy flux, q_i is given by:

$$q_i = -\lambda \frac{\partial T}{\partial x_i} + \rho \sum_{k=1}^{N_{sp}} h_k Y_k V_{k,i} \tag{5}$$

where, λ stands for the translational temperature diffusion coefficient and $\sigma_{ij} = \tau_{ij} - p\delta_{ij}$.

2.2. NRP discharge model

Numerical studies based on detailed plasma chemistry have shown that in NRP discharges characterized by a reduced electric field, E/N, in the range of 150 to 400 Townsends, the discharge energy is mainly stored in electronic and vibrational excited states of molecules. Following this result, during the pulse characteristic time, τ_d, we assume that the discharge energy is deposited into two components of the gas energy: vibrational and electronic energies. Two source terms are considered:

$$\dot{S}^p_{ET}(t_{per}, x_i) = \begin{cases} \alpha \cdot \frac{\sigma_{pulse}}{\tau_d} \cdot \mathcal{F}(x_i) & \text{if } t_{per} \leq \tau_d \\ 0 & \text{if } t_{per} > \tau_d \end{cases} \tag{6}$$

and

$$\dot{S}^p_{vib}(t_{per}, x_i) = \begin{cases} (1-\alpha) \cdot \frac{\sigma_{pulse}}{\tau_d} \cdot \mathcal{F}(x_i) & \text{if } t_{per} \leq \tau_d \\ 0 & \text{if } t_{per} > \tau_d \end{cases} \tag{7}$$

where S^p_{ET} and S^p_{vib} are the source terms of the gas electronic and vibrational energy, respectively. α is the model parameter that represents the fraction of the discharge energy going into electronic states, whereas (1-α) refers to the fraction going into vibrational states. σ_{pulse} refers to the discharge energy density (J/m3) deposited per pulse during the time period, τ_d. t_{per} refers to the time in the pulse referential. The function $\mathcal{F}$ spatially defines where the plasma discharge occurs and is modeled as follows:

$$\mathcal{F}(x_i) = erfc\left(\frac{r(x_i)}{a}\right)^b \tag{8}$$

where $r(x_i)$ refers to the radius of the discharge channel and a and b are geometric parameters. So far, the above presented set of governing equations, Eq. (1-4), do not account for these vibrational and electronic states of molecules. However, these molecules will eventually relax into thermal equilibrium in a given characteristic relaxation time, as described next.

2.3. ***Ultra-fast phenomena:*** *relaxation of electronic states of molecules within a characteristic time of tens of nanoseconds*

Experimental [6, 7] and numerical works [8] have shown that the fraction of the discharge energy stored in electronic states of N_2 molecules results in the production of atomic oxygen and in gas heating within 50 nanoseconds, through dissociative quenching reactions with molecular oxygen:

$$N_2(X) + e^- \rightarrow N_2(A, B, C, a', ...) + e^- \tag{9}$$

$$N_2(A, B, C, a', ...) + O_2 \rightarrow 2O + heat \tag{10}$$

This two-step mechanism, which is an extension of the one proposed by [8] is known as the ultra-fast gas heating phenomenon. Experimental studies of [9, 3], have also corroborated this rapid formation of atomic oxygen and temperature increase during the discharge characteristic time. In these works, not only the ultra-fast mechanism is pointed as the dissociative mechanism but also the direct impact of electrons with O_2 molecules is considered:

$$O_2 + e^- \rightarrow 2O + e^- \tag{11}$$

Meaning that the source term $\dot{S}^p_{ET}$ defined in Eq. (6) may be directly added to the gas total energy equation Eq. (4), as long as the model ensures that part of this energy is routed to the dissociation of molecular oxygen, as experimentally observed:

$$\frac{\partial(\rho e)}{\partial t} + \frac{\partial(\rho u_i e)}{\partial x_i} = -\frac{\partial q_i}{\partial x_i} + \frac{\partial}{\partial x_i}(\sigma_{ij} u_i) + \dot{S}^p_{ET} \tag{4a}$$

An additional molar production rate term for both oxygen and molecular oxygen species is modeled as follows:

$$\dot{\omega}^p_O = \eta_{diss} \cdot \frac{\sigma_{pulse}}{\tau_d \cdot h^o_O} \cdot \frac{Y_{O_2}}{Y^{air}_{O_2}} \qquad \text{if } t_{per} \leq \tau_d \tag{12}$$

$$\dot{\omega}^p_{O_2} = -\frac{W_O}{W_{O_2}} \cdot \dot{\omega}^p_O \qquad \text{if } t_{per} \leq \tau_d \tag{13}$$

$$\dot{\omega}^p_k = 0 \qquad \text{if } \quad k \neq \mathrm{O}, \mathrm{O}_2 \tag{14}$$

where η_{diss} is an empirical parameter of the model that corresponds to the fraction of the discharge energy going into O_2 dissociation. h^o_O stands for the molar enthalpy of formation of atomic oxygen . $Y^{air}_{O_2}$ refers to the O_2 mass fraction in air and the ratio $Y_{O_2}/Y^{air}_{O_2}$, on the RHS of Eq. (12), ensures that the dissociation rate of O_2 tends to zero when all dioxygen is consumed. W_O and W_{O_2} stand for the atomic and molecular oxygen molar

masses. The model assumes a single channel for the production of atomic oxygen through the dissociation of molecular oxygen. Note that only the fraction of the discharge energy going into O_2 dissociation is considered, it does not distinguish the physical mechanism that gives rise to O atoms, either through electrons direct impact with O_2 molecules or quenching reactions as such of the ultrafast heating mechanism may be considered as ultrafast dissociation mechanisms of O_2 molecules. The model for the ultrafast dissociation of O_2 molecules, Eqs.(12-14), is added to the corresponding species balance equation, Eq. (3):

$$\frac{\partial(\rho Y_k)}{\partial t} + \frac{\partial}{\partial x_i}(\rho(u_i + V_{k,i})Y_k) = W_k\dot{\omega}_k^c + W_k\dot{\omega}_k^p \qquad (3a)$$

*2.4. **Slow phenomena:** relaxation of vibrational states of molecules within a characteristic time from microseconds to miliseconds.*

The discharge energy stored in vibrational levels of N_2 molecules [8, 10, 11] will eventually reach thermal equilibrium with translational mode. According to [12], vibrational states of N_2 molecules may last for a long period of time in the mixture before an equilibrium is reached between vibrational and translational modes. The authors derived an empirical correlation to compute the vibrational-translational relaxation time of excited N_2 molecules by the k^{th} collisional species partner, τ_{VT}^k, as a function of the local gas composition and the mixture temperature:

$$\tau_{VT}^k = c/p_k \cdot exp\left(a_k \cdot (T^{-1/3} - b_k) - 18.42\right) \qquad (15)$$

where k^{th} refers to O_2, O and N_2. $c = 1$ (atm.s), p_k is the partial pressure of the k^{th} species and a_k and b_k are experimental constants depending on the k^{th} species. An additional transport equation for the gas vibrational energy is introduced:

$$\frac{\partial(\rho e_{vib})}{\partial t} + \frac{\partial(\rho u_i e_{vib})}{\partial x_i} = \frac{\partial}{\partial x_i}\left(\rho\mathcal{D}\frac{\partial e_{vib}}{\partial x_i}\right) + \dot{S}_{vib}^{\,p} - \dot{R}_{VT}^p \qquad (16)$$

where $\dot{S}_{vib}^{\,p}$ corresponds to the energy deposited over vibrational modes of molecules during the discharge pulse as defined in Eq. (7). The first term on the RHS of Eq. (16) refers to the diffusion of the vibrational energy, where the diffusion coefficient of nitrogen, $\mathcal{D} = \mathcal{D}_{N_2}$, is considered. $\dot{R}_{VT}^p$ is the vibrational energy relaxation rate. This term models the energy exchange rate between vibrational and translational mode. It is modeled considering the Landau-Teller harmonic oscillator approach:

$$\dot{\mathrm{R}}_{VT}^p = \rho\frac{e_{vib} - e_{vib}^{eq}(T)}{\tau_{VT}} \qquad (17)$$

in which, the equilibrium value of the vibrational energy at a given mixture temperature, $e_{vib}^{eq}(T)$, is defined as:

$$e_{vib}^{eq}(T) = \frac{r \cdot \Theta_1}{e^{\Theta_1/T} - 1}, \text{ with } \Theta_1 = 3396 \text{ K} \qquad (18)$$

where with $\Theta_1 = 3396$ K is the vibrational temperature corresponding to the first quantum vibrational state and $r = R/W_{N_2}$, with R the gas constant and W_{N_2} the nitrogen molar mass. τ_{VT}, is computed as a function of τ_{VT}^k given by the experimental correlation of [12], Eq. (15):

$$\tau_{VT} = \left(\frac{1}{\tau_{VT}^O} + \frac{1}{\tau_{VT}^{O_2}} + \frac{1}{\tau_{VT}^{N_2}}\right)^{-1} \qquad (19)$$

This model only considers a single vibrational level of molecules and therefore vibrational-vibrational energy exchanges are not considered. By energy conservation, the relaxation of vibrational energy corresponds to an increase of gas temperature and therefore, to an overall increase of gas total energy. In this sense, the relaxation source term in Eq. (16) should be added to the gas total energy balance equation, Eq. (4a):

$$\frac{\partial(\rho e)}{\partial t} + \frac{\partial(\rho u_i e)}{\partial x_i} = -\frac{\partial q_i}{\partial x_i} + \frac{\partial}{\partial x_i}(\sigma_{ij}u_i) + S_{ET}^{\,p} + \dot{R}_{VT}^p \qquad (4b)$$

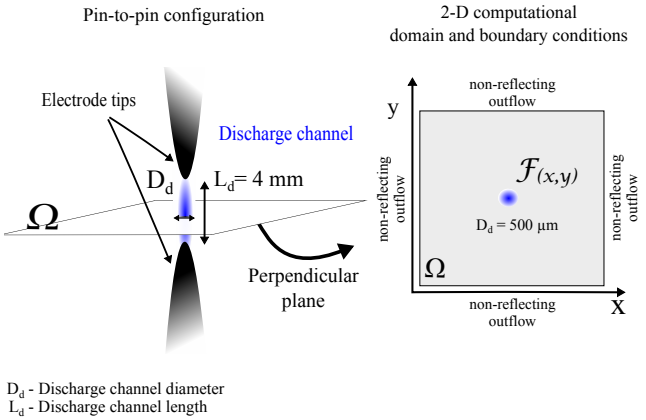

Figure 1: Schematics of a pin-to-pin configuration of NRP discharges device. The 2-D computational domain is a plane perpendicular to the electrode tips.

3. Numerical Method

The present model is implemented in a structured Direct Numerical Simulation solver dedicated to compressible reactive flow simulations with detailed chemistry [5]. The spatial derivatives are computed with a 4^{th} order centered finite-difference scheme. An 8^{th} order filtering scheme is used for stability purpose. The code is explicit in time using a 4^{th} order Runge-Kutta method. To capture stiff pressure waves induced by the plasma discharge, the hyper-viscosity technique developed in [13] is employed.

The numerical configuration is shown in Fig. 1. The plasma discharge channel is assumed cylindrical with diameter D_d and height L_d. When $D_d/L_d << 1$, both the temperature and species axial gradients are neglected as in [14], and a 2-D computational domain, perpendicular to the electrode tips, may be considered as shown in Fig. 1. The computations are performed on a uniform mesh grid with a cell size of 10×10 μm.

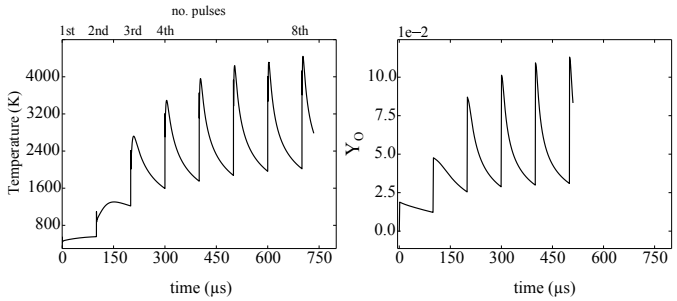

Figure 2: Temporal evolution of gas temperature and atomic oxygen mass fraction in a sequence of NRP discharges in air. f = 10 kHz, energy per pulse = 650 μJ, model parameters: α = 0.55 and η_{diss} = 0.35.

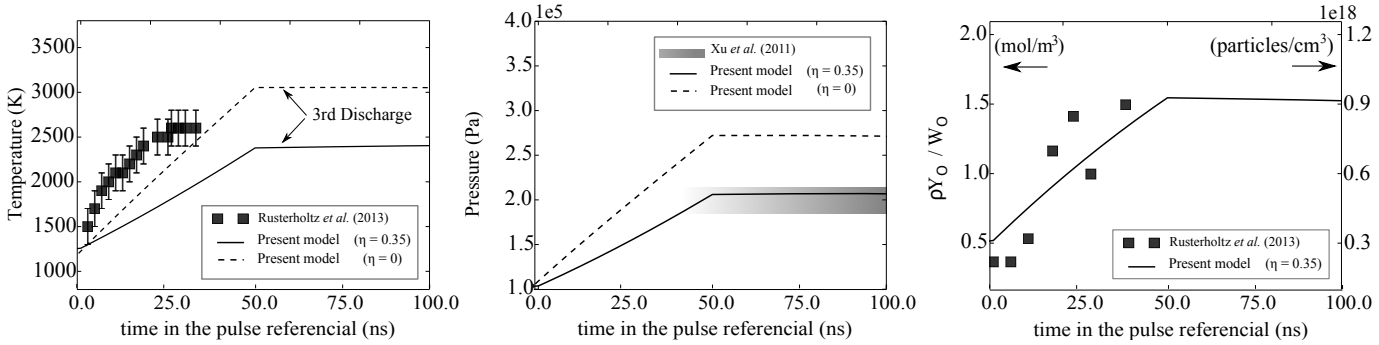

Figure 3: Temporal evolution of maximum value of gas temperature, pressure and concentration of atomic oxygen during the 3^{rd} discharge pulse. Model results are compared to experimental results obtained in [7].

4. Results and discussion

4.1. NRP discharges in air

Figure 2 shows the temporal evolution of the gas temperature and atomic oxygen mass fraction in a sequence of NRP discharges in air with pulse frequency, f = 10 kHz and pulse energy 650 μJ and discharge radius, r = 250 μm. Model parameters are α = 0.55 and η = 0.35. By construction, during the ultra-fast characteristic time, 35% of the discharge energy goes into the dissociation of O_2 molecules into O atoms. The evolution of Y_O shown in Fig. 2 is explained by the evolution of the gas temperature inside the discharge zone at the beginning of each discharge. As Fig. 2 shows, the gas temperature at the beginning of the first four pulses, increases with the number of discharges from T = 300 to 2000 K approximately, reaching a more stationary regime after the 6^{th} pulse when the diffusive effects compensate the fast increase of temperature during the discharge. These results are in good agreement with numerical results presented in [14] where a detailed plasma kinetic model was considered, and also with the experimental results obtained in [7]. In Fig. 3 the evolution of the gas temperature, pressure and O atoms concentration, during the 3^{rd} pulse, are plotted against the experimental data of [7]. Two values of the model parameter η are analyzed. For the reference value, where η is set to 0.35, during the pulse, pressure rises up to 2 atm, temperature increases about 1100 K and O atoms concentration rises from 0.3 up to 0.9e18 particles/cm^3 showing a good agreement with experimental results. When η is set to 0, the gas pressure rises up to 2.8 atm and the temperature increases about 1800 K, overestimating the experimental results. In this case, no model of O_2 dissociation is considered, O radical is not formed during the pulse as only a result of the gas temperature and pressure increase. This shows that in order to capture O atoms formation during the plasma discharge, the dissociation model presented above is needed on top of the conventional reaction mechanism model. Compressible effects occur at each discharge. For a better understanding of this phenomena, Fig. 4 shows the temporal evolution of gas pressure radial profiles following the 3^{rd} discharge for the same two values of η. After the fast increase of the pressure, at t = 0.2 μs, gas expands and an initial shock wave propagates outwards through the surrounding air. As energy source ceases after the pulse characteristic time, the shock strength diminishes both from the expansion and from viscous dissipation. Eventually the shock decays into a sound wave, propagating with the speed of sound. This means that due to these pressure waves created by the plasma discharge, part of the deposited energy leaves the discharge zone as acoustic energy. For η = 0.35 about 10% of the pulse energy is converted into acoustic energy, whereas for η = 0 this value increases to about 20%, (results not shown here). These results confirm that the discharge energy going into gas chemical energy will not be lost as acoustic energy and, therefore, the energy runaway from the discharge zone during gas expansion is minimized. This also impacts on the relaxation of vibrational energy. As expected from Eq. (2.4), Fig. 5 shows that the relaxation of the gas vibrational energy into gas heating is more effective when O_2 dissociation is considered during the discharge, η = 0.35.

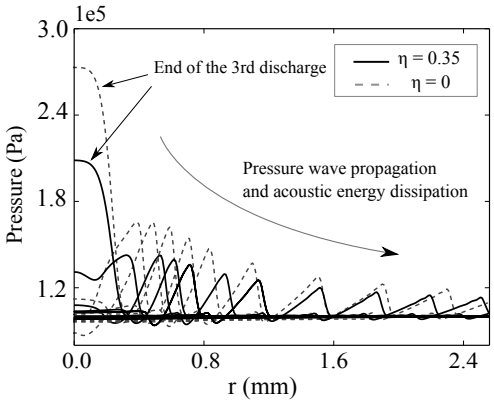

Figure 4: Temporal evolution of the pressure radial profiles after 3rd discharge pulse, two values of the model parameter η are shown: $\eta = 0$ and $\eta = 0.35$.

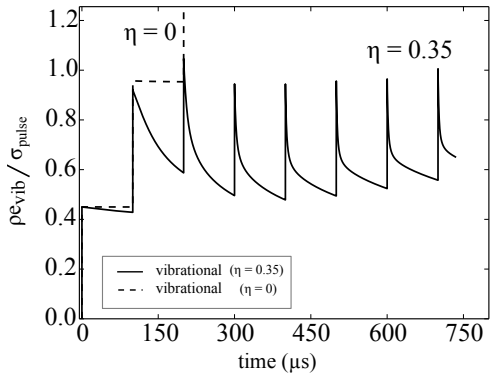

Figure 5: Temporal evolution of gas vibrational energy in a sequence of NRP discharges in air, two values of the model parameter η are considered.

In this case, after the 3^{rd} pulse, most of the vibrational energy deposited during a pulse is relaxed before the next one. On the other hand, for $\eta = 0$, gas vibrational energy and will not contribute to the increase of gas temperature and, therefore, to ignition.

4.2. Methane-air mixture ignition - Quiescent flow conditons

NRP discharges are applied into a methane-air mixture characterized by an equivalence ratio $\phi = 0.8$. The initial gas temperature is T = 300 K and the mixture is at rest. Figure 6 shows the temporal evolution of the major species mass concentration at the centre of the discharge channel for the above two values of η. In the reference case where η is set to 0.35, the results show that during the ultra-fast characteristic time, along with O atoms, CH_2O, HCO, H_2O and other intermediate combustion species are formed. This means that O atoms are fast recombined initiating branching reactions. Eventually the radicals formed during the first pulse are recombined to form CO_2 and H_2O which are much more stable species that last until the second pulse. As it can be seen, CH_2O and CH_3O mass concentration also increases at the center of the discharge channel. On the other hand, O atoms and OH are fast recombined between 2 pulses. Nevertheless, regarding CH_4 mass concentration, combustion has barely started during the first pulse and only at the second discharge, the concentration of CH_4 diminish consistently, leading to an effective ignition event. For $\eta = 0$, the results shows that although an higher increase of gas temperature during τ_d, intermediate combustion species only become significant after the 3rd discharge pulse as a consequence of the strong temperature increase. These results show a major contribution of O atoms on mixture ignition. If O atoms are not formed, four discharge pulses are needed to ignite the mixture along with a much higher value of the gas temperature than the reference case.

4.3. Methane-air mixture ignition - Turbulent flow conditions

Although turbulence does not have an effect during the discharge time (τ_d = 50 ns), results show that it modifies all the scalar fields in between discharges. Scalar fields are modified between two consecutive pulses due to turbulence, leading to a non-homogeneous distribution of the gas temperature as well as radicals inside the discharge zone. Figure 7 shows that the gas vibrational energy is also convected due to turbulence towards regions where gas temperature and O atoms concentration are too low to induce its relaxation into gas heating. Depending on the pulse repetition frequency these turbulent fluctuations may lead to the failure of ignition. Indeed, in high turbulent flow Reynolds number, the hot-spot formed during the pulse may be convected and engulfed by the surrounding fresh gases. It follows that the thermochemical conditions inside the discharge zone for the next pulse might be similar to those of the previous one and therefore, the cumulative effect of repetitively discharges on the mixture ignition may become negligible. For the present turbulent Reynolds number, three to five discharges were needed to ignite the mixture. This confirms that flow field characteristics should be taken into account when computing a train of NRP discharges in reactive mixtures and need to be considered in LES and RANS NRP discharges-assisted combustion models.

5. Conclusions

We have constructed a model to simulate the impact of short pulses electric discharges on gas temperature and species dissociation in order to study the phenomena of NRP discharges-assisted ignition. DNS results of a train of NRP discharges in air show a good agreement with the experimental results. Ignition phenomena through NRP discharges results in quiescent and turbulent flows show that part of the pulse energy remains stored as vibrational energy up to ignition. On the other hand, the cumulative effect of gas temperature and radicals concentration increase, inside the discharge zone as a result of the repetitiveness of pulses, leads to ignition. We have show that O_2 dissociation contributes more effectively to the ignition phenomena than the temperature increase and also that with the increase of turbulence inside the discharge zone the number of discharges needed to ignite the mixture increases.

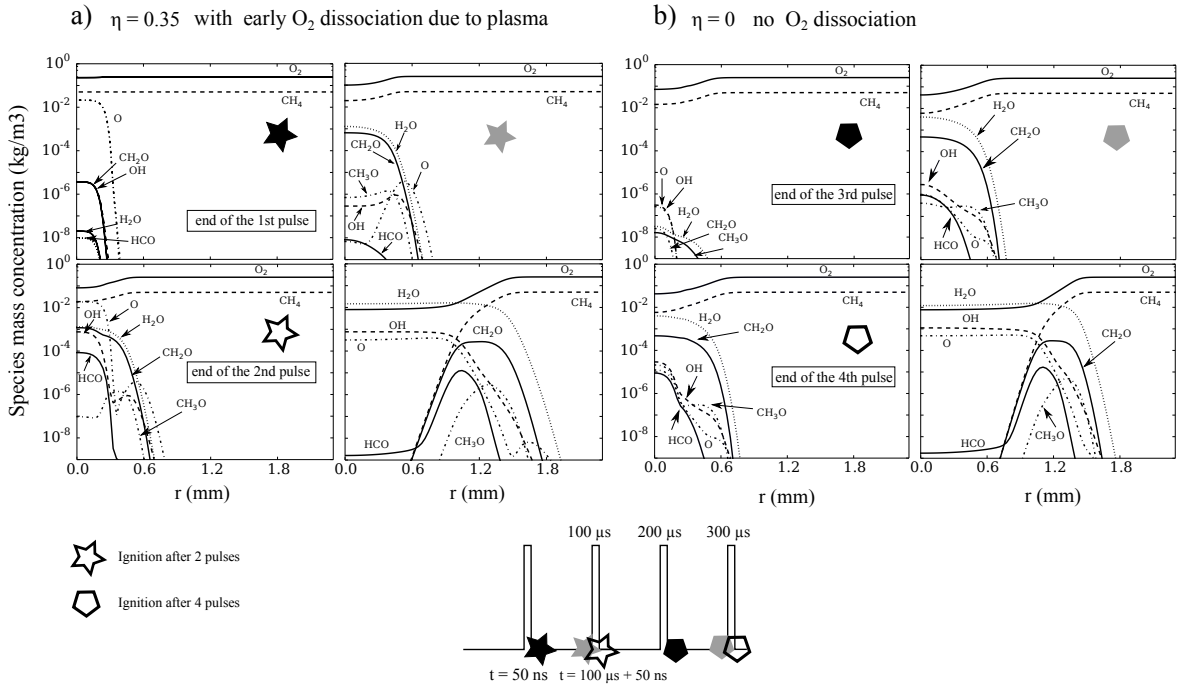

Figure 6: Radial profiles of major species density for 4 different instants, two values of the model parameter η are considered.

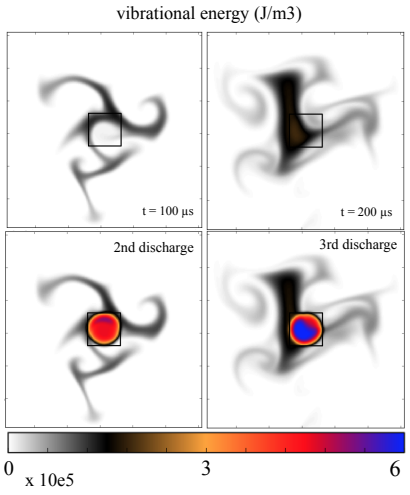

Figure 7: Impact of the turbulence on the gas vibrational energy field, in two consecutive pulses.

6. Acknowledgements

This research has been supported by Agence Nationale de la Recherche FAMAC project (Grant no. ANR-12-VPTT-0002) and PLASMAFLAME project (Grant no. ANR-11-BS09-0025) and was performed using HPC resources from GENCI-IDRIS.

References

[1] G. Pilla, D. Galley, D. A. Lacoste, F. Lacas, D. Veynante, C. Laux, Plasma-enhanced combustion of a lean premixed air-propane turbulent flame using a repetitively pulsed nanosecond discharge., Plasma Science, IEEE Transactions on 34 (2006) 2471–2477.

[2] W. Kim, H. Do, M. G. Mungal, M. A. Cappelli, A study of plasma-stabilized diffusion flames at elevated ambient temperatures, Combustion and Flame 153 (2008) 603–615.

[3] I. V. Adamovich, I. Choi, N. Jiang, J.-H. Kim, S. Keshav, W. R. Lempert, E. Mintusov, M. Nishihara, M. Samimy, M. Uddi, Plasma Sources Science and Technology 18 (2009) 034018.

[4] A. Starikovskiy, N. Aleksandrov, Progress in Energy and Combustion Science 39 (2013) 61 – 110.

[5] A. Coussement, O. Gicquel, J. Caudal, B. Fiorina, G. Degrez, Three-dimensional boundary conditions for numerical simulations of reactive compressible flows with complex thermochemistry, Journal of Computational Physics 231 (2012) 5571 – 5611.

[6] G. D. Stancu, F. Kaddouri, D. A. Lacoste, C. O. Laux, Atmospheric pressure plasma diagnostics by oes, crds and talif, Journal of Physics D: Applied Physics 43 (2010) 124002.

[7] D. L. Rusterholtz, D. A. Lacoste, G. D. Stancu, D. Z. Pai, C. O. Laux, Journal of Physics D: Applied Physics 46 (2013) 464010.

[8] N. Popov, Investigation of the mechanism for rapid heating of nitrogen and air in gas discharges, Plasma Physics Reports 27 (2001) 886–896.

[9] M. S. Bak, M. G. M. H. Do, M. A. Cappelli, Plasma-assisted stabilization of laminar premixed methane/air flames around the lean flammability limit, Combustion and Flame 159 (2012) 3128 3137.

[10] A. Flitti, S. Pancheshnyi, Gas heating in fast pulsed discharges in n2-o2 mixtures, The European Physical Journal 45 (2009) 21001.

[11] N. L. Aleksandrov, S. V. Kindysheva, M. M. Nudnov, A. Y. Starikovskiy, Mechanism of ultra-fast heating in a non-equilibrium weakly ionized air discharge plasma in high electric fields, Journal of Physics D: Applied Physics 45 (2009) 21001.

[12] R. C. Millikan, D. R. White, Systematics of vibrational relaxation, Journal Chemical Physics 39 (1963) 3209–3213.

[13] B. Fiorina, S. K. Lele, An artificial nonlinear diffusivity method for supersonic reacting flows with shocks, Journal of Computational Physics (2007) 246–264.

[14] G. V. Naidis, Simulation of spark discharges in high-pressure air sustained by repetitive high-voltage nanosecond pulses, Journal of Physics D: Applied Physics 41 (2008) 234017.